JCTC Journal of Chemical Theory and Computation

Article

pubs.acs.org/JCTC

Analytical Gradients for the MSINDO-sCIS and MSINDO-UCIS Method: Theory, Implementation, Benchmarks, and Examples

Immanuel Gadaczek,* Katharina Krause, Kim Julia Hintze, and Thomas Bredow

Mulliken Center for Theoretical Chemistry, Institut für Physikalische und Theoretische Chemie, Universität Bonn, Beringstr. 4, 53115 Bonn, Germany

Supporting Information

ABSTRACT: Analytical expressions for the sCIS (scaled configuration interaction singles) and UCIS (unrestricted CIS) energy gradients are presented for the semiempirical method MSINDO. The theoretical background of the derivation of the analytical gradients is presented, and the implementation into the MSINDO program package is described. The computational efficiency of the underlying *Z*-vector method is greatly enhanced by making use of the transpose-free quasiminimal residual (TFQMR) algorithm. Benchmark timing tests are compared to the widely used TD-B3LYP approach. For a statistical evaluation of the accuracy of MSINDO-sCIS, geometry optimizations are performed for a small set of organic molecules in selected excited states. The obtained results are compared to CASPT2 and TD-B3LYP/TZVP. In order to demonstrate the applicability of the present approach to periodic systems within the cyclic cluster model, we present first calculations of the excited state structure of ethyne adsorbed on the NaCl (100) surface.

1. INTRODUCTION

The accurate description of excited-state geometries is still challenging for quantum chemistry. Despite the urgent demand in the determination of excited states properties in areas ranging from photochemistry to spectroscopy and biology,[1,2] current state-of-the-art quantum chemical methods are still not applicable to the large and complex systems that are of interest here.[3] A particular case is fluorescent molecules, which are of wide interest in science, technology, and industrial applications. Photovoltaic cells, organic light emitting diodes (OLEDs), and diagnostic probes in biology and medicine are only a few examples of their applications.[4] For optimal performance, flourescent molecules have to fulfill a number of conditions, such as minimal overlap between absorption and emission bands, large quantum yields, and photochemical stability. For quantum chemists, the understanding and prediction of the optical and spectroscopic properties of these dyes are major tasks.

From the theoretical point of view, it would be desirable if excited-state geometry optimizations of large molecules could be carried out by current state-of-the-art methods, i.e., coupled-cluster (CC),[5−9] multistate complete active space perturbation theory of second order (MSCASPT2),[10] or multireference configuration interaction (MR-CI).[11] However, due to their unfavorable scaling, these methods cannot be applied to molecules with more than a few atoms.[12] The most popular approach for molecules with up to ∼200 atoms is time-dependent density functional theory (TD-DFT),[13−15] which has been extensively used for the calculation of excited states over the past decade. Unfortunately, TD-DFT has problems in the description of Rydberg-valence states and charge-transfer (CT) states.[16,17] The CT problem is inherent to DFT due to the self-interaction error and is even not fully remedied by the so-called double-hybrid methods,[18,19] where an MP2 (Møller−Plesset second order) correction is introduced to correct the energy. Since CT states play an important role in the mechanisms of fundamental processes in photovoltaic cells, e.g., electron−hole formation and separation, TD-DFT is not expected to describe organic solar cell devices correctly. Only the so-called range-separated or long-range corrected density functionals, which have been developed in the past decade, show a reliable $1/R$ behavior,[20,21] while the common hybrid functionals still fail. In order to investigate processes in technological applications, the development of a method which is still affordable for more than 1000 atoms without showing a CT error is desirable. For the calculation of large systems, semiempirical methods have provided good reliability.[22,23] We have recently shown that the semiempirical MSINDO-sCIS method (modified symmetric orthogonalized intermediate neglect of differential overlap with scaled configuration interaction singles),[24−27] which is related to Zerner's INDO approximation,[28−30] leads to reasonable results for vertical excitation energies of molecules and also shows a correct $1/R$ behavior for CT states.[31] This approach includes an improvement of the CIS excitation energies by a semiempirical correction, which can be seen as a simplified CIS(D)[32,33] method. Additionally, this method has been applied to periodic systems using the cyclic cluster model (CCM),[34] and it has been shown recently that it correctly describes excited states in solids and surfaces providing[35] an alternative to the computational highly costly GW approximation.[36,37] The next logical step is the implementation of an analytical energy gradient for the MSINDO-sCIS method to get access to excited-state equilibrium structures, vibronically coupled electronic spectra and reaction mechanisms in photochemistry, and molecular dynamics on excited-state potential energy surfaces.

The derivation and implementation of CI derivatives is well documented in the literature for several types of closed- and open-shell CI wave functions.[38−43] The main feature in the

Received: December 2, 2011
Published: January 30, 2012

   dx.doi.org/10.1021/ct200867n | J. Chem. Theory Comput. 2012, 8, 986−996

calculation of the gradient is that after the CI eigenvalues have been obtained, only the calculation of density matrices and the orbital relaxation contribution has to be carried out. The orbital relaxation contribution can be calculated by solving the coupled-perturbed Hartree−Fock equations (CPHF)[44] and can be computed in a much more efficient manner by the Z-vector approach[45] of Handy and co-workers.[46,47] These techniques implementations have also been implemented into other semiempirical methods. A very successful approach has been developed by Thiel in NDDO based[48] configuration interaction (CI) methods.[49]

In this paper, we derive the analytical gradient for the MSINDO-sCIS and MSINDO-UCIS approaches, in a way similar to the CIS gradient derived by Pople and his group before.[50] However, here we use configuration state functions to form directly spin-pure eigenstates. For the unrestricted CIS method (UCIS), it is well-known that spin-contamination plays an important role.[51] But in order to provide a complete set of methods for both open- and closed-shell cases, we derived also the UCIS equations and implemented them to the MSINDO program package. After a short review of the theory, we show an efficient way to solve the CPHF equations to obtain the Z-vector and give a short overview of the implementation strategies. Then, we present benchmark results for the computational timings. In order to check the accuracy of the method, we calculated the S_1 structures of a small set of organic closed- and open-shell molecules. Followed by a statistical evaluation, we close the paper with an example of excited-state optimization of adsorbed ethyne on the NaCl(100) surface employing periodic boundary conditions via the CCM.[34]

2. COMPUTATIONAL METHODS

In this section, we describe the derivation of the analytical gradients of the MSINDO-sCIS excited state energies. Since the derivation is well-known and described in detail in the literature,[50,52] we will just point out the major changes. A detailed description of the derivation for both, restricted and unrestricted, cases is given in the Supporting Information. Furthermore, the implementation of a fast linear equation system solver is briefly discussed, which is used for the solution of the CPHF equations. The MSINDO-sCIS energy can be expressed for both spin cases—singlet and triplet—through the following equation:

$$E_{\mathrm{sCIS}} = E_{\mathrm{HF}} + \sum_{ij}^{\mathrm{occ}} \sum_{ab}^{\mathrm{vir}} t_i^a t_j^b [(\varepsilon_a - \varepsilon_i)\delta_{ab}\delta_{ij} + 2c_1(ia|jb) - c_2(ij|ab)] \quad (1)$$

In the case of singlet excitations, c_1 and c_2 are given in ref 31; for triplets, it is $c_1 = 0$ and $c_2 = c_T$ from ref 31. In the original implementation, the additional empirical correction term d_{ia}^{corr} is used in the diagonal elements of the sCIS matrix. The corresponding contributions are neglected in the implementation of the analytical gradient, since they are zero for excited states, which do not belong to a total symmetric irreducible representation. In premliminary test calculations, it was found that changes in the geometries of total symmetric states are below 0.1%. Additionally, the explicit derivation of this term leads to a slower convergence behavior in the geometry optimization. Only for the converged structure is d_{ia}^{corr} used for the determination of the excited state energy. This leads to a higher computational efficiency, because the arising additional terms in the Lagrangian and the two-particle density matrix do not have to be calculated.

During the derivation of the excited state gradient, the expression for the analytical gradient is split into the MO response part and the derivatives with respect to the basis functions. For the MO-response part, the common ansatz of unitary transformation of the orbitals is used. Since the overlap matrix is the unity matrix in MSINDO, the derivatives of the overlap and also the calculation of the energy-weighted overlap vanish. Therefore, the only nonvanishing part of the MO response is given by the virtual-occupied part of the Lagrangian:

$$\begin{aligned} L_{ai} = & \sum_{jk}^{\mathrm{occ}} D_{jk}[4(ai|jk) - (aj|ik) - (ij|ak)] \\ & + \sum_{bc}^{\mathrm{vir}} D_{bc}[4(ai|bc) - (ab|ic) - (ib|ac)] \\ & + 2\sum_{b}^{\mathrm{vir}} t_i^b \sum_{j}^{\mathrm{occ}} \sum_{c}^{\mathrm{vir}} t_j^c [2c_1(ab|jc) - c_2(aj|bc)] \\ & - 2\sum_{j}^{\mathrm{occ}} t_j^a \sum_{k}^{\mathrm{occ}} \sum_{b}^{\mathrm{vir}} t_k^b [2c_1(ji|kb) - c_2(jk|ib)] \end{aligned} \quad (2)$$

and the unknown virtual-occupied parts of the transformation matrix $\mathbf{U}^y$, which are solved by the coupled-perturbed Hartree−Fock equations using the common Z-vector approach.[45−47] For the solution of the resulting system of linear equations, the transpose-free quasi-minimum residual algorithm (TFQMR) by Freund[53] for the iterative solution is used. Only matrix-vector operations are taken into account. For a detailed description, see ref 53. We will just give the needed vectors for this algorithm in this paper. The required parts are the Lagrangian and a σ vector which is defined by $\mathbf{AZ}$ (for details, see the Supporting Information). For the sCIS case, the σ vector is given by

$$\sigma_{jb}^{\mathrm{sCIS}} = (\varepsilon_b - \varepsilon_j)Z_{bj} + \sum_{i}^{\mathrm{occ}} \sum_{a}^{\mathrm{vir}} [4(ia|jb) - (aj|ib) - (ab|ij)]Z_{ai} \quad (3)$$

While the sCIS-σ vector uses spatial orbitals in this equation, for the UCIS case, spin orbitals have to be considered (see the Supporting Information).

All integrals are calculated in the AO basis, and the resulting MO dependent terms are transformed back into the AO basis, when they are needed. The Z-vector equations are solved completely in the MO basis, since the solution is basis independent. This reduces the computational effort. For details of the calculation of all terms, see the Supporting Information. All terms have been brought to a matrix form that allows an efficient use of the BLAS libraries.[54,55] Considering the INDO approximation, where only derivatives of two-electron−two-center integrals of the type $(\mu\mu|\nu\nu)$ are present, the two-particle density becomes a two-dimensional matrix. For the sCIS case, the two-particle density matrix is given by

$$\Gamma_{\mu\nu} = 2c_1 T_{\mu\mu}T_{\nu\nu} - c_2 T_{\mu\nu}T_{\mu\nu} + P_{\mu\mu}^{\mathrm{sCIS}}P_{\nu\nu}^{\mathrm{HF}} - \frac{1}{2}P_{\mu\nu}^{\mathrm{sCIS}}P_{\mu\nu}^{\mathrm{HF}} + \frac{1}{2}P_{\mu\mu}^{\mathrm{HF}}P_{\nu\nu}^{\mathrm{HF}} - \frac{1}{4}P_{\mu\nu}^{\mathrm{HF}}P_{\mu\nu}^{\mathrm{HF}} \quad (4)$$

dx.doi.org/10.1021/ct200867n | J. Chem. Theory Comput. 2012, 8, 986−996

where $P_{\mu\nu}^{sCIS}$ is the relaxed excited state density without the ground state density. Since the nonrelaxed densities (those where the MO response is not included) are needed for the calculation of the Lagrangian, they are calculated before the TFQMR algorithm is started. After the TFQMR algorithm has converged, the densities are combined to represent the full one- and two-particle densities. This must be done because the ground-state density is included in the one-particle density after the calculation of the two-particle density Γ. With these two densities, the gradient can be calculated in the following way:

$$\frac{dE_{sCIS}}{dy} = \sum_{\mu\nu} P_{\mu\nu}^{\Delta} h_{\mu\nu}^{(y)} + \sum_{\mu\nu} \Gamma_{\mu\nu}(\mu\mu/\nu\nu)^{(y)} + V_{NN}^{(y)} \quad (5)$$

where the fully relaxed sCIS density $\mathbf{P}^{\Delta}$ is given by $\mathbf{P}^{HF} + \mathbf{P}^{sCIS}$. Since this equation is the same for the sCIS and the UCIS cases, the same subroutines can be used in MSINDO. With the calculated gradient, the geometry relaxation step can be done, and the geometry optimization of any selected state can be carried out.

3. CALCULATION TIMINGS

To test the performance and the computational efficiency of the gradient calculation, we calculated a series of linear connected polycyclic aromatic hydrocarbons. In Figure 1a, we have plotted the calculation timings for the main steps and the overall process. In the overall process, we estimated that the gradient calculation is an $O(N^{2.8})$ process. The most time-consuming process in the calculation of the gradient is the calculation of the *Z*-vector via the iterative TFQMR algorithm. Convergence is reached if a change in the residual is below 10^{-12}. This is the defined standard value in MSINDO, but it can be changed as needed. From Figure 1b, it can be seen that the number of iterations required for TFQMR convergence has an $O(N^{0.5})$ dependency on the system size. The calculation of the integral derivatives is done in a loop over atom pairs. Those are calculated in an internal coordinate system and are transformed back to the global coordinate system before the gradient is evaluated. At first glance, this seems to be inefficient, but the derivatives of the Coulomb and one-electron integrals can be calculated much faster than in the global coordinate system by exploiting local symmetry. The CPU time ratio between the calculation of the excited state vector and the corresponding gradient depends on the excited state S_n or in general X_n. This can be explained as follows. The higher the index *n* is, the more excited states have to be calculated within the Davidson algorithm,[56,57] which is implemented for the excited-state calculation.[31] The calculation of the excited-state gradient does not depend on such a variable and, therefore, in all cases only depends on the convergence behavior of the TFQMR algorithm. Since this is only depending on the system size, the calculation of the X_n gradient can be seen as constant for a given molecule. For the lower excited states, the ratio between the evaluation time of the excited-state vectors and that of the corresponding gradient is up to 60 (see Table 1).

Table 1. MSINDO-sCIS Computational Performance for the Lowest Singlet Excited State S_1 for Linear Polycyclic Aromatic Hydrocarbons $C_{4m+2}H_{2m+4}$[a]

$N_{electrons}$	$t(E_{sCIS})$	$t(dE_{sCIS}/dy)$	$t(dE_{TD\text{-}B3LYP}/dy)$
48	0.25	0.02	212.11
66	0.41	0.04	540.17
84	2.56	0.09	1216.88
102	4.93	0.14	1594.72
120	6.17	0.17	2496.36
138	13.00	0.31	3611.40
156	16.68	0.38	4866.33
174	20.63	0.55	6719.16
192	26.85	0.71	9040.85
210	36.05	0.90	11808.16
228	45.52	1.19	17428.57
246	50.55	1.58	24508.78
264	60.53	1.78	46639.18

[a]All calculation timings are given in seconds. The number of electrons correponds to the number of valence electrons, which are explicitly taken into account in MSINDO.

In order to further accelerate the excited-state geometry optimization, the CIS vectors of the previous step are used as the new guess vectors in the actual step. As the geometry relaxation steps are usually small, the changes in the $|\Psi_I\rangle$'s are

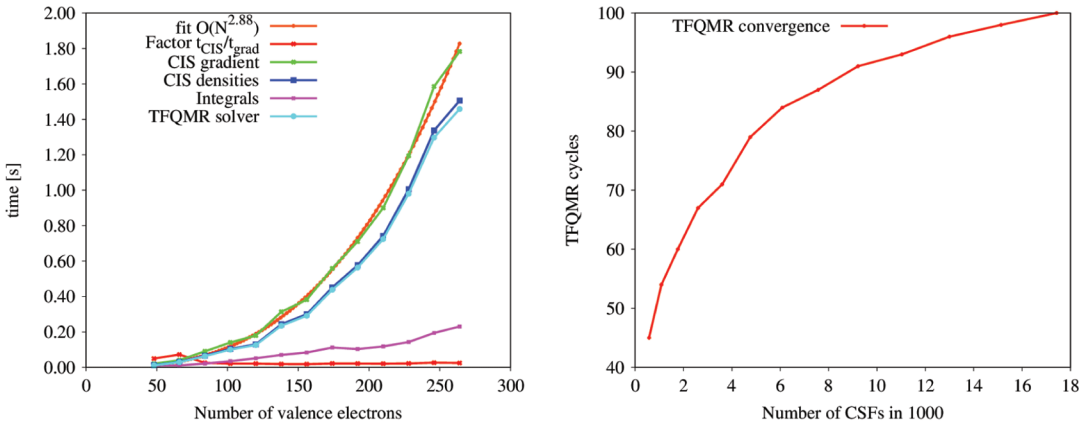

(a) (b)

Figure 1. Computational statistics for the current implementation of the sCIS and UCIS gradient in MSINDO. (a) Total timing for the gradient calculation decomposed into the different parts. The time for the calculation of the densities includes the TFQMR calculation. (b) The number of TFQMR iterations depending on the number of unknowns, which is in the special case of CIS theory the number of all excited states in one molecule. All calculations where carried out on an Intel Core 2 Duo E8400 CPU with 3.00 GHz.

small, too. This leads to a fast convergence of the Davidson algorithm in the excited state calculations after the zeroth geometry optimization step. A corresponding technique was implemented for the *Z*-vector, which leads to a faster convergence in the TFQMR algorithm after the zeroth geometry optimization step. For a better comparison with more common methods for excited-state calculations, we benchmarked the CPU timings of our method against the TD-B3LYP method with a TZVP basis set. The TD-DFT calculations have been carried out using the ORCA program package,[58,59] which is designed for the calculation of spectroscopic molecular properties. A comparison between MSINDO-sCIS and TD-B3LYP for the CPU time necessary for a gradient calculation is given in Table 1. As expected, the semiempirical approach is 3−4 orders of magnitude faster than the first-principles method. Also, the scaling behavior of the MSINDO-sCIS gradient calculation is slightly better than for the TD-B3LYP calculation.

4. BENCHMARK CALCULATIONS

The molecules used in this benchmark study refer to the reference set selected by the CASPT2 study of Page and Olivucci.[60] The optical excitations of these molecules can be regarded as representatives of typical $n-\pi^*$ or $\pi-\pi^*$ transitions. The set of molecules consists of acroleine, acetone, the propenoic acid anion, and diazomethane as representatives of $n-\pi^*$ transitions and *E*-butadiene, *Z*-butadiene, and pyrrole as representatives of $\pi-\pi^*$ transitions. For a further analysis, the original reference set has been expanded by three more chromophores belonging to the class of protonated Schiff bases that represent $\pi-\pi^*$ transitions. These chromophores have been used as model systems in a previous theoretical study of the structure relaxation in the excited state of 11-*cis*-retinal with CASSCF, CASPT2, CC, and QMC.[61] The same reference set has been used before to benchmark TD-DFT excited-state geometry optimizations.[62] According to the TD-DFT study by Guido et al., we label the protonated Schiff bases as model B (MDB), model C (MDC), and model D (MDD), see Figure 2. In our study, we use the CASPT2 results as a theoretical reference and discuss the quality of the MSINDO-sCIS results in comparison to the TD-DFT results. To demonstrate that the MSINDO-sCIS parametrization does not have the same problems with ground-state geometries as INDO/S,[63] we start with their statistical evaluation. Afterward, we will describe the excited-state geometries in detail and evaluate the statistical parameters.

4.1. Ground-State Geometries. Ground-state structures of a large set of molecules have been studied with MSINDO before, see ref 31 and references therein. First, we discuss the ground-state structures of the benchmark set of Page and Olivucci.[60] As the present study is mainly on excited-state structures, we will just give the statistical evaluation of the different bond types and angles. The structural parameters of the different benchmark molecules are given in Table 8 in the Supporting Information. In Table 2, we report the statistical parameters for this small benchmark set. It can be seen that all double bonds are slightly underestimated by MSINDO, while single bonds are slightly overestimated. Comparing these values to the B3LYP standard given in ref 62 (0.013−0.024 Å for single and 0.006−0.008 Å for double bonds), it is obvious that MSINDO performs quite similarly, except for the angles, where MSINDO is slightly worse than B3LYP. This shows that MSINDO is well parametrized for the ground state.

Table 2. MSINDO-sCIS Deviations from CASPT2 Ground-State Geometries for the Benchmark Set of Page and Olivucci[60] (Bond Lengths in Å and Angles in Degrees)

parameter	*N*	mean	abs. mean	max	std. dev.
C−C	6	0.012	0.016	0.038	0.021
C═C	6	−0.017	0.017	−0.025	0.020
C═O	3	−0.002	0.005	−0.008	0.006
C═N	1	−0.008	0.008	−0.008	
angles	11	0.675	1.388	3.601	1.866

4.2. MSINDO-sCIS Excited-State Geometries. *Acetone.* The first excited state of acetone is the A_2 state corresponding to a $n-\pi^*$ transition. The structural parameters can be found in Table 3. The adiabatic excitation energy E_{0-0} of 4.12 eV is slightly overestimated by 0.21 eV compared to the CASPT2 reference. This value is of similar quality to the TD-B3LYP result, which however underestimates the E_{0-0} value by 0.28 eV. The structure of this excited state is reproduced in a similar way as with TD-B3LYP. While the C═O bond is underestimated by more than 0.1 Å, the C−C bond is well

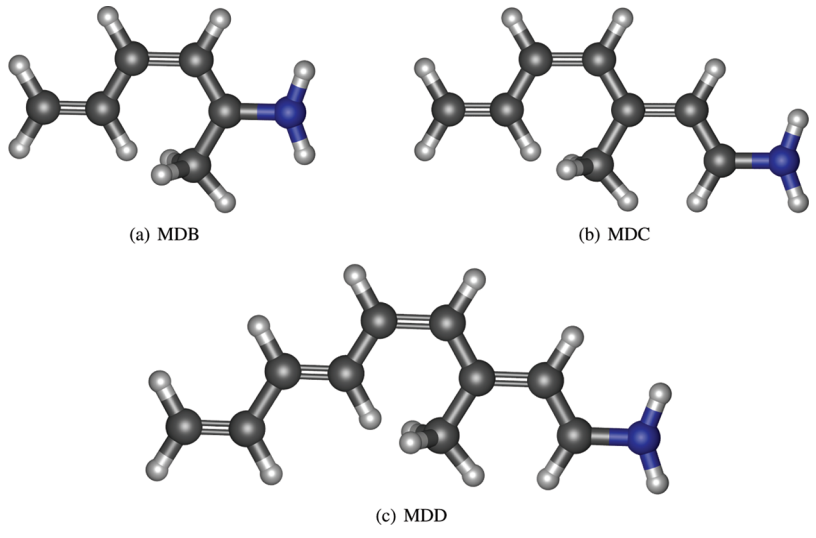

Figure 2. Used protonated Schiff bases in the benchmark study.

Table 3. S_1 Excited State Geometries, Bond Lengths in Å, Angles in Degrees, and Adiabatic Excitation Energies in eV (Values in Parentheses Are the Difference from the CASPT2 Reference)

molecule	state	parameter	MSINDO-sCIS[a]		TD-B3LYP[b]		reference[c]
acetone	A_2	E_{0-0}	4.12	(0.21)	3.65	(−0.28)	3.93
		C═O	1.266	(−0.102)	1.331	(−0.037)	1.368
		C−C	1.504	(0.015)	1.497	(0.008)	1.489
		∠(OCC)	120.2	(3.2)	117.8	(0.8)	117.0
acroleine	A''	E_{0-0}	3.37	(0.19)	2.84	(−0.34)	3.18
		C═O	1.259	(−0.018)	1.225	(−0.052)	1.277
		C_1−C_2	1.463	(0.034)	1.437	(0.008)	1.429
		C_2═C_3	1.333	(−0.017)	1.345	(−0.005)	1.350
		∠(*OCC*)	125.2	(−0.2)	130.7	(5.3)	125.4
		∠(CCC)	122.0	(−0.5)	123.0	(0.5)	122.5
diazomethane	A_2	E_{0-0}	3.16	(0.52)	2.52	(−0.12)	2.64
		N═N	1.206	(−0.009)	1.205	(−0.010)	1.215
		C═N	1.256	(−0.071)	1.305	(−0.022)	1.327
propenoic acid anion	A''	E_{0-0}	3.41	(−0.08)	1.49	(−1.98)	3.47
		C−O_1	1.259	(−0.013)	1.293	(0.021)	1.272
		C═O_2	1.249	(−0.145)	1.295	(−0.099)	1.394
		C_1−C_2	1.534	(0.133)	1.424	(0.023)	1.401
		C_2═C_3	1.374	(−0.035)	1.415	(0.006)	1.409
		∠(OCC)	116.8	(−0.5)	126.2	(8.9)	117.3
		∠(CCC)	118.3	(−8.4)	125.1	(−1.6)	126.7
		∠(OCO)	138.3	(26.5)	107.4	(−4.4)	111.8
E-butadiene	B_u	E_{0-0}	5.35	(−0.83)	4.93	(−1.25)	6.18
		C_2−C_3	1.407	(0.008)	1.404	(0.005)	1.399
		C_1═C_2	1.388	(−0.033)	1.424	(0.003)	1.421
		∠(CCC)	123.3	(−0.8)	123.9	(−0.2)	124.1
Z-butadiene	B_2	E_{0-0}	5.28	(−0.31)	4.13	(−1.46)	5.59
		C_2−C_3	1.406	(0.008)	1.406	(0.008)	1.398
		C_1═C_2	1.388	(−0.033)	1.420	(−0.001)	1.421
		∠(CCC)	126.0	(4.0)	121.8	(−0.2)	122.0
pyrrole	B_2	E_{0-0}	5.56	(−0.67)	5.54	(−0.69)	6.23
		N−C_1	1.412	(−0.004)	1.394	(−0.022)	1.416
		C_1═C_2	1.428	(−0.033)	1.450	(−0.011)	1.461
		C_2−C_3	1.380	(0.010)	1.369	(−0.001)	1.370
		∠(CNC)	105.2	(−2.1)	105.9	(−1.4)	107.3
		∠(NCC)	109.8	(1.7)	108.5	(0.4)	108.1
		∠(CCC)	107.6	(−0.6)	108.0	(−0.2)	108.2
MDB	A'	E_{0-0}	4.97	(1.25)	3.91	(0.21)	3.72
		N═C	1.381	(0.014)	1.346	(−0.021)	1.367
		C_1−C_2	1.421	(−0.026)	1.484	(0.037)	1.447
		C_2═C_3	1.435	(0.003)	1.376	(−0.056)	1.432
		C_3−C_4	1.408	(−0.022)	1.460	(0.030)	1.430
		C_4═C_5	1.375	(−0.021)	1.384	(−0.012)	1.396
		C_1−C_6	1.476	(−0.023)	1.490	(−0.009)	1.499
		∠(NC_1C_6)	118.3	(0.7)	118.3	(0.7)	117.6
		∠($C_3C_4C_5$)	121.0	(−0.1)	123.5	(2.4)	121.1
MDC	A'	E_{0-0}	3.81	(0.66)	3.27	(0.12)	3.15[d]
		N═C	1.367	(0.015)	1.336	(−0.016)	1.352
		C_1−C_2	1.403	(−0.019)	1.425	(0.003)	1.422
		C_2═C_3	1.422	(0.003)	1.383	(−0.036)	1.419
		C_3−C_4	1.416	(−0.039)	1.496	(0.041)	1.455
		C_4═C_5	1.412	(0.004)	1.375	(−0.033)	1.408
		C_5−C_6	1.424	(−0.008)	1.448	(0.016)	1.432
		C_6═C_7	1.357	(−0.025)	1.372	(−0.010)	1.382
		C_3−C_8	1.483	(−0.023)	1.496	(−0.010)	1.506
		∠(NC_1C_2)	123.4	(1.5)	122.3	(0.4)	121.9
		∠($C_5C_6C_7$)	121.7	(1.7)	122.1	(2.1)	120.0
MDD	A'	E_{0-0}	3.35	(0.94)	2.79	(0.38)	2.41
		N═C	1.371	(0.019)	1.337	(−0.015)	1.352
		C_1−C_2	1.390	(−0.023)	1.414	(0.001)	1.413
		C_2═C_3	1.418	(0.004)	1.387	(−0.027)	1.414

dx.doi.org/10.1021/ct200867n | J. Chem. Theory Comput. 2012, 8, 986−996

Table 3. continued

molecule	state	parameter	MSINDO-sCIS[a]		TD-B3LYP[b]		reference[c]
		C_3-C_4	1.413	(−0.041)	1.483	(0.029)	1.454
		$C_4=C_5$	1.414	(0.011)	1.362	(−0.041)	1.403
		C_5-C_6	1.404	(−0.027)	1.463	(0.032)	1.431
		$C_6=C_7$	1.392	(−0.005)	1.371	(−0.026)	1.397
		C_7-C_8	1.436	(0.008)	1.439	(0.011)	1.428
		$C_8=C_9$	1.348	(−0.027)	1.367	(−0.008)	1.375
		C_3-C_{10}	1.483	(−0.024)	1.502	(−0.005)	1.507
		$\angle(NC_1C_2)$	123.9	(1.4)	122.8	(0.3)	122.5
		$\angle(C_7C_8C_9)$	122.6	(0.8)	123.8	(2.0)	121.8

[a]Present work. [b]Taken from ref 60; if not there, from ref 62. [c]Taken from ref 62. [d]Taken from ref 61.

reproduced with an overestimation of 0.015 Å. For this molecule, TD-B3LYP is more accurate in the structure description, since it underestimates the C=O bond length by only 0.037 Å and overestimates the C−C bond by only 8 mÅ. The ∠(OCC) is much more strongly overestimated by MSINDO-sCIS than by TD-B3LYP (120.2° vs 117.8° compared to the reference of 117.0°).

Acroleine. Acroleine belongs to point group C_s and shows a $n-\pi^*$ transition with A'' symmetry as the S_1 state (see Table 3). Again, the E_{0-0} energy is overestimated with MSINDO-sCIS. This overestimation (by 0.17 eV) is less pronounced than the underestimation obtained with TD-B3LYP (0.34 eV), and even the structural parameters are similar to the TD-B3LYP S_1 geometry. The underestimation of the C=O bond of 0.018 Å is smaller with TD-B3LYP (0.052 Å). But the different C−C and C=C bond lengths obtained with MSINDO-sCIS have a much larger variation from the CASPT2 reference than those of TD-B3LYP (see Table 3). The angles are slightly underestimated by MSINDO-sCIS, while TD-B3LYP overestimates the bond angles.

Diazomethane. The zwitterionic species diazomethane maintains the C_{2v} symmetry in the excited state. The adiabatic excitation energy of the S_1 state with A_2 symmetry corresponding to a $n-\pi^*$ transition is overestimated by 0.52 eV with MSINDO-sCIS. Here, TD-B3LYP is more accurate, with an underestimation of only 0.12 eV. Since no angles are present in the benchmark set, we can only discuss the bond lengths. The N=N bond length is well reproduced with both MSINDO-sCIS and TD-B3LYP (1.206 Å and 1.205 Å compared to the CASPT2 value of 1.215 Å). But the C=N double bond is strongly underestimated by 0.071 Å. This effect can be explained by the missing C=N bonding situation in the reference set,[31] which is used in the parametrization.

Propenoic Acid Anion. The last representative of an $n-\pi^*$ transition is the propenoic acid anion, where the S_1 state has a A'' symmetry. The adiabatic excitation energy is near to the CASPT2 value (3.41 eV vs 3.47 eV). This is considerably better than the TD-B3LYP result, which underestimates this value by nearly 1.5 eV (see Table 3). This effect can be explained by the charge-transfer (CT) character of the excited state. It is well-known that TD-DFT does not accurately describe CT states,[16] and it has been demonstrated that this is not the case for MSINDO-sCIS.[31] Surprisingly, the S_1 structure obtained with TD-DFT calculated is quite close to the CASPT2 structure. Here, the description via MSINDO-sCIS fails for the ∠(OCC) bonding angle (error of 26.5°). This is the outlier in the benchmark set and the maximum error for angles. This problem may be due to a wrong description of the charge delocalization over the carboxylacid group.

E-Butadiene. The S_1 state of *E*-butadiene has a B_u symmetry. This is the first representative of $\pi-\pi^*$ transitions in our small benchmark set. Although MSINDO-sCIS underestimates the adiabatic excitation energy by 0.83 eV (5.35 eV compared to 6.18 eV from CASPT2), this error is still smaller than the error of TD-B3LYP (Δ = 1.25 eV). The value of the single C−C bond length is closer to CASPT2 than the C=C double bond value. Here, we find a discrepancy with TD-B3LYP, since MSINDO-sCIS underestimates the double bond by 0.033 Å, whereas TD-B3LYP overestimates it by 3 mÅ. The differences in the ∠(CCC) angles are below 1° and therefore in good agreement with the CASPT2 reference.

Z-Butadiene. The structural isomer of *E*-butadiene is *Z*-butadiene, which belongs to the C_{2v} point group. The S_1 state is a $\pi-\pi^*$ transition of B_2 symmetry. Again, TD-B3LYP fails in the quantitative description of the adiabatic excitation energy. The CASPT2 value of 5.59 eV can be reproduced within a reasonable error range by MSINDO-sCIS (5.28 eV, Δ = −0.31 eV), whereas TD-B3LYP strongly underestimates the value by 1.46 eV. Since for both *E*- and *Z*-butadiene molecules the S_1 state has no CT character, the failure of TD-B3LYP can only be explained by basis set effects. These effects have been observed before for vertical excitation energies.[64] The same structural effects as for *E*-butadiene can be observed for *Z*-butadiene within the MSINDO-sCIS calculation. The C=C bond length is more underestimated (Δ = −0.033 Å) than the single bond length (Δ = 0.008 Å). But here, the ∠(CCC) angle is overestimated by 4.0°.

Pyrrole. The B_2 symmetric $\pi-\pi^*$ transition in pyrrole is the S_1 state of this molecule. Considering the structural parameters (see Table 3), it can be seen that MSINDO-sCIS performs similarly to TD-B3LYP. The adiabatic excitation energy is underestimated for both methods by nearly the same amount (errors are −0.67 eV and −0.69 eV). Also, the N−C single bond lengths are similar (1.412 Å and 1.394 Å compared to the reference of 1.416 Å), while the length of the C=C double bond is less underestimated by TD-B3LYP (errors of −0.011 Å for TD-B3LYP and −0.033 Å for MSINDO-sCIS). All angles are within an acceptable error range (0.6−2.1° for MSINDO-sCIS vs 0.2−1.4° for TD-B3LYP) and behave identically in over- and underestimation.

Protonated Schiff Bases (PSB). The S_1 states of all three molecules are formed by a $\pi-\pi^*$ transition with A' symmetry. The numbering of the carbon atoms (see Table 3) starts with the carbon bonded to the nitrogen and is continued along the chain except the methyl group. This carbon atom of the methyl group always has the highest number. The adiabatic excitation energies are strongly overestimated by MSINDO-sCIS with errors between 0.66 and 1.25 eV. The error is larger than with

Table 4. MSINDO-UCIS Values (Denoted as UCIS) for Excited-State Structural Parameters of the Two Radicaloic Peroxyethylene Isomers[a]

	trans-isomer				*cis*-isomer			
	D_1, A'		D_2, A'		D_1, A'		D_2, A'	
parameter	UCIS	ref	UCIS	ref	UCIS	ref	UCIS	ref
$\langle S^2 \rangle$	0.793		1.292		0.791		1.313	
E_{0-0}	0.805	0.791	2.747	4.243	0.787	0.660	3.639	4.181
O−O	1.405	1.448	1.296	1.449	1.406	1.440	1.238	1.448
O−C_1	1.395	1.385	1.364	1.379	1.388	1.375	1.405	1.384
C_1−C_2	1.340	1.363	1.355	1.538	1.333	1.363	1.337	1.545
C_1−H_{gem}	1.098	1.077	1.098	1.072	1.103	1.078	1.095	1.073
C_2−H_{trans}	1.071	1.081	1.073	1.077	1.070	1.081	1.079	1.078
C_2−H_{cis}	1.071	1.081	1.073	1.072	1.070	1.079	1.079	1.076
∠(OOC_1)	102.6	107.6	137.6	108.0	106.7	110.1	129.3	111.1
∠(OC_1C_2)	117.7	119.4	121.3	111.2	130.1	127.2	124.1	122.7
∠($C_1C_2H_{cis}$)	121.3	125.0	121.2	129.0	121.8	123.2	120.9	121.5
∠($C_1C_2H_{trans}$)	119.6	118.8	119.7	119.7	119.4	117.9	121.7	117.8
∠($C_2C_1H_{gem}$)	126.4	121.8	126.1	119.0	126.4	124.7	124.7	126.3

[a]Comparison is made to highly correlated ab initio methods taken from ref 66. Energies in eV, distances in Å, and angles in degrees.

TD-B3LYP, where deviations of only 0.12 up to 0.38 eV are observed. But the MSINDO-sCIS structural parameters are in better agreement with the CASPT2 references than with TD-B3LYP. In particular, the ∠(CCC) angles show very small errors compared to the TD-B3LYP results. The values for the C═N bond lengths are quite similar with those of MSINDO-sCIS (Δ between 0.014 and 0.019 Å) and TD-B3LYP (Δ between 0.012 and 0.021 Å). For the C−C and C═C bonds, the error increases with the distance to the nitrogen. The errors for the single bonds (|Δ| between 0.023 and 0.026 Å for MDB, 0.019 and 0.039 Å for MDC, and between 0.008 and 0.041 Å for MDD) are larger than for the C═C double bonds (|Δ| between 0.003 and 0.021 Å for MDB, 0.003 and 0.025 Å for MDC, and between 0.004 and 0.024 Å for MDD with increasing distance to the nitrogen atom). The error for the C-methyl bond is nearly constant in all three molecules (−0.023 Å), whereas TD-B3LYP varies within a smaller error range (0.005 to 0.010 Å).

4.3. MSINDO-UCIS Excited State Geomerties of Radicalic Systems. For the evaluation of excited-state geometries of open-shell molecules, we have chosen a rather small benchmark set. This is due to the lack of an extended benchmark set for open-shell molecules to our knowledge. Considering that UCIS is not able to describe the geometries of excited states correctly due to the spin contamination,[51] the only reference which is expected to accurately describe excited state geometries of open-shell molecules is CASSCF or MCSCF, since these methods provide spin-pure states. For TD-UDFT, it is still not clear why excited states of open-shell molecules are not as accurate as for the closed-shell case,[65] since no extensive benchmark set is available. Therefore, it is really not possible to asses the effect of ground state spin contamination on the quality of the excited state geometry in the case of TD-DFT. Therefore, we have restricted our benchmark to two well-studied molecules. This set consist of the *cis*- and *trans*-peroxyethylene radicals. We calculated the equilibrium geometries of the first two excited states. The energy surfaces of these systems are in fact quite complicated. Therefore, we selected the reference state using three different criteria: the symmetry of the state, the multiplicity of the state, and the best comparison for the geometry. In agreement with the MCSCF results of Krauss et al.,[66] MSINDO-UHF favors the *trans*-isomer energetically by less than 0.05 eV. The structures of the first two excited states of both radicaloid systems are given in Table 4. The ground-state structures can be found in Table 9 in the Supporting Information. Therein, we denote C_1 as the carbon bonded to the peroxylene group and the geminal hydrogen H_{gem} as the hydrogen atom bonded to the same carbon. The distinction between the *cis*- and *trans*-hydrogens, both bonded to C_2, depends on the positioning to the peroxylene group. To distinguish between the *cis*- and *trans*-isomers of the molecule, we have chosen the positioning around the central oxygen, according to the MCSCF reference.[66] No spin-pure excited states have been obtained by a MSINDO-UCIS calculation. Although we observe a spin-contamination, we denote the given excited state in Table 4 as doublets with the symbol D_i.

Ground-State Structures. Since this paper does not aim at ground-state structures, we will not compare MSINDO-UHF and MCSCF results in detail. Only a brief overview will be given here. All numerical values for the ground state are given in Table 9 in the Supporting Information. The values for bonds and angles are in a reasonable error range. The largest errors were observed for the O−O bond distances, where the errors are between 0.077 (*trans*) and 0.075 (*cis*) Å, and the ∠(OOC_1) angle (Δ = 2.4° for *trans* and Δ = 2.6° for *cis*). This is due to the missing radicaloid peroxycarbon systems in the reference set, which has been used in the parametrization of MSINDO. The remaining bonds and angles are within the typical error range of semiempirical methods.

trans-Peroxyethylene Radical. The first excited state of the *trans*-isomer has an adiabatic energy of 0.791 eV and has A' symmetry. MSINDO-UCIS reproduces this energy with only a small error of 0.014 eV. The geometry of this excited state is qualitatively well reproduced. The O−O bond is slightly underestimated by 0.043 Å, which is less than for the ground state. Opposite to this, the O−C bond is slightly overestimated by 0.01 Å, which is also less than for the ground state. Unfortunately, this does not hold for the C−C bonding distances, whose underestimation is enlarged compared to the ground state (Δ = 0.023 Å) but still within a reasonable error range. The C−H_{gem} bond is overestimated 0.018 Å and the C−$H_{cis,trans}$ bonds are underestimated by 0.01 Å. Although this error is

Table 5. Deviations of the Different Structural Parameters for MSINDO-sCIS (Denoted as sCIS) and TD-B3LYP (Denoted as B3LYP) Compared to the CASPT2 Reference Set[a]

		mean		abs. mean		±max		std. dev.	
parameter	N	sCIS	B3LYP	sCIS	B3LYP	sCIS	B3LYP	sCIS	B3LYP
ΔE_{0-0}	10	−0.188	0.543	0.562	0.681	1.250	−1.980	0.704	0.972
C−C	18	−0.003	0.013	0.027	0.015	0.133	0.041	0.040	0.021
C═C	15	−0.014	−0.018	0.018	0.019	−0.035	−0.056	0.022	0.026
C═O	3	−0.088	−0.063	0.088	0.063	−0.145	−0.099	0.126	0.083
C═N	4	−0.006	−0.019	0.030	0.019	−0.071	−0.022	0.044	0.022
angles	17	1.6	0.9	3.2	1.9	26.5	8.9	7.1	3.0

[a]Bond lengths are given in Å, angles in degrees, and energies in eV.

rather small, the difference in over- and underestimation leads to a different order compared to MCSCF. The angles for this excited-state geometry are described qualitatively correctly with larger errors if oxygen atoms involved. The errors are between 0.8 and 5.0°.

The second excited state of the *trans*-peroxyethylene radical is of A'' symmetry, with an adiabatic excitation energy of 2.747 eV, which is 1.496 eV below the MCSCF result. We attribute this large error to the much higher spin contamination compared to the ground state ($\langle S^2\rangle$ of 1.292 vs 0.793). This indicates that higher excitations play an important role[51] in the calculation of this state. In the MCSCF reference, it can be seen that the excitation breaks the C═C double bond (1.355 Å for MSINDO-UCIS and 1.538 Å for MCSCF), since there is the largest change in the interatomic distances. Although we optimized the geometries of all excited states below 7 eV, we could not observe any state where this kind of excitation was observed. All other values for the interatomic distances are in a good agreement with the reference (|Δ| between 0.001 and 0.026 Å). The wrong behavior for the spin distribution into the O−O bond yields a wrong behavior for the $\angle(OOC_1)$, too. Here, we find the largest outlier, where the angle is enlarged to 137.6°, which is not observed in the reference ($\angle(OOC_1)$ = 108.0°). The same observation was made for the $\angle(OC_1C_2)$, whose value is significantly larger than in the reference, while all other angles are better reproduced with errors between 0.0° and 7.1°. From our point of view, the phenomenon of a wrong description of the excited state originates from a high spin contamination, which is rather inherent to the UCIS approach than due to semiempirical approximations.

cis-Peroxyethylene Radical. Analogous to the *trans*-isomer, the first two excited states in the *trans*-peroxyethylene radical are of A'' and A'' symmetry. The adiabatic excitation energy of the first excited state (A') is well reproduced with an overestimation of 0.127 eV (0.787 vs 0.660 eV). Qualitatively, the same results were observed for the *cis* form as for the *trans* form. The O−O bond distance is well reproduced with an error of −0.034 Å (see Table 4). Nearly the same underestimation was obtained for the C−C bond (Δ = −0.030 Å), while the C−O bond is slightly overestimated by 0.013 Å. Again, the optimized MSINDO-UCIS structure has a wrong ordering for the C−H interatomic distances, with an overestimation of the $C-H_{gem}$ bond (Δ = 0.025 Å) and an underestimation of the $C-H_{cis,trans}$ bonds (Δ = −0.006 Å for $C-H_{trans}$ and Δ = −0.009 Å for $C-H_{cis}$, respectively). The angles are in good agreement with the MCSCF reference. Again, the errors are large if the angles involve oxygen atoms (|Δ| between 2.9 and 3.6°). While the ∠(OOC) angle is underestimated, the ∠(OCC) angle is overestimated by nearly the same amount. The $\angle(CCH_i)$ angles are in a reasonable error range below 2.0° (Δ = −1.4° for $\angle(CCH_{cis})$, Δ = −1.5° for $\angle(CCH_{trans})$ and Δ = 1.7° for $\angle(CCH_{gem})$).

The second excited state (A'' with a reference E_{0-0} value of 4.181 eV) is underestimated by MSINDO-UCIS for the adiabatic excitation energy (E_{0-0} = 3.639 eV, Δ= 0.542 eV). This is not as strong as for the *trans* form, but here we observe the same problems as for the *trans*-isomer. The C−C bond distance shows the largest deviation from the reference state with 0.209 Å. All interatomic distances between C and H are reasonably described with errors below 0.022 Å. The $O-C_1$ bond is slightly overestimated by 0.019 Å, but the O−O bond is strongly underestimated by 0.21 Å, again. This underestimation is larger than for the *trans*-isomer, but the error for the $\angle(OOC_1)$ is lower (18.2°). The other angles are acceptable but have a larger spread than for the *trans* form. The errors are between and 0.4° and 3.9°. Also in this case, we explain these large errors with the much higher spin-contamination in this excited state compared to the ground state. This means that higher excitations have to be included to get the description of this state correct.[51]

4.4. Statistical Evaluation. *MSINDO-sCIS.* For the statistical evaluation of the accuracy of MSINDO-sCIS for excited states, we distinguish between the different bond types, angles, and adiabatic excitation energies. The results are shown in Table 5. The adiabatic excitation energies ΔE_{0-0} calculated via the MSINDO-sCIS method are similar to or even slightly better in all statistical aspects than the values obatained by TD-B3LYP. The same observation is made for C═C double bonds. Here, MSINDO-sCIS is similar to TD-B3LYP within the standard deviation. In the case of C−C single bonds, MSINDO-sCIS shows less accurate results compared to TD-B3LYP, but the values are still in a reasonable range; the lengths of C═O bonds are in all cases underestimated as for TD-B3LYP. But the mean errors are still reasonable and only slightly larger than for TD-B3LYP. The last bond type which is discussed in the benchmark set is the C═N bond. Here, MSINDO-sCIS is comparable to TD-B3LYP. The outlier is still in the mÅ region, which shows how well the method is parametrized for this kind of bonding in the excited state. For all angles which were considered in the benchmark set, MSINDO-sCIS performs reasonably except for the already discussed outlier in the propionic acid. This large error of 26° strongly affects the statistics, since the number of considered values is still low.

MSINDO-UCIS. Different from the statistical evaluation for the MSINDO-sCIS method, we do not separate the different bond types due to the small number of reference values. We have calculated two different values for each statistical property. The first value includes all measured bonds and angles, while the second one—denoted with parentheses in Table 6—excludes the O−O bonds and the ∠(OOC) angles, because

dx.doi.org/10.1021/ct200867n | J. Chem. Theory Comput. 2012, 8, 986−996

Table 6. Deviations of the Calculated Structural Parameters Obtained with MSINDO-UCIS Compared to the MCSCF Reference Set[a]

parameter	bonds	angles	ΔE_{0-0}
N	24 (20)	20 (16)	4
mean	−0.033 (−0.018)	2.83 (1.08)	−0.474
abs. mean	0.045 (0.032)	5.35 (3.18)	0.544
std. dev.	0.081 (0.065)	8.99 (4.37)	0.921
± max	−0.210 (−0.208)	29.60 (10.10)	−1.496

[a]The values in parentheses denote the statistical values without consideration of the O−O bonds and ∠OOC angles. Bond lengths are given in Å, angles in degrees, and energies in eV.

radicaloid peroxyl groups have not been included in the reference set, which was used in the parametrization. Without these bond types, MSINDO-UCIS shows reasonable behavior for the angles, with mean absolute errors of 3.2° and an only slightly larger standard deviation. The same holds for the bonds, where the statistical errors are below 0.05 Å, as long as no peroxyl bonds are considerated. This is different if the O−O bonds are included. The change for the maximum deviation is only very small, since we cannot reproduce the excited state, where the C−C bond is enlarged. Unfortunately, no systematical studies of unrestricted TD-DFT optimization are present in the literature, so that we cannot give a comparison to common methods. The energies differ dramatically from the CASSCF reference if the excited states are higly spin-contaminated. Here, a maximum underestimation of nearly 1.5 eV is obtained with a high standard deviation of 0.9 eV, although the absolute mean value is about 0.5 eV. It must be concluded from our results that the highly complicated potential energy hypersurfaces of open-shell molecules in their excited states cannot be described by this simple approach. This is due to the high spin contamination, which is also present in the ab intio CIS approach for unrestricted determinants. Therefore, in future work, we plan to introduce a spin-projection in the ground state to reduce the spin contamination, which would lead to a new semiemprical method for excited states of open-shell molecules, which is as reliable as the MSINDO-sCIS method. Although it is well-known that the restricted open-shell ansatz for configuration interaction singles yields spin-pure excited states, it has been demonstrated by Maurice and Head-Gordon, that this approach is not always reliable and can give wrong results if higher excitations play an important role.[51] In those cases, the $\langle S^2 \rangle$ value of the UCIS excited state can be an indicator. If the spin contamination in the excited state is higher than for the ground state, higher excitations play a more important role and have to be included.[51] This problem might not be solved in the same way as for the MSINDO-sCIS method, where a reparameterization has significantly improved the results.[31] Additionally, a reformulation of the CIS problem within the spin-flip approach could be possible.[67] The SF-CI model can describe within a single-reference formalism some inherently multireference situations, such as single bond-breaking and diradicals.[68−70] This could be an option to solve the problem with the wrong energies. Further work on that problem is in progress.

5. APPLICATION TO ADSORPTION ON SURFACES

MSINDO allows for periodic calculations by the use of the cyclic cluster model.[34] Therefore, it is easy to implement the analytical sCIS gradient for the periodic calculation. The implementation is done by a simple weighting scheme at the borders, which has been described before.[35] As an illustrative example, we will describe in this section the S_1 structure of adsorbed ethyne on the NaCl(100) surface. To our knowledge, no experimental data are available for this system and no other theoretical examination of this system has been carried out before. A graphical overview of this photochemical experiment is given in Figure 3 and will be described in detail in the following paragraphs. Although the equilibrium S_1 structure of the free ethyne molecule is C_{2h} symmetric,[71,72] the adsorbed species does not have the chance to order itself in that way on the surface. The structure where the molecular mirror plane is ordered parallel to the NaCl(100) surface is not even a local minumum due to the repulsive interaction of one hydrogen with the surface. Also, the ground-state structure is of C_{2v} symmetry if the ethyne is adsorbed (see Figure 3a). In the ground state, the ethyne is placed with the C−C bond above the Na atom of the surface with the C−H bonds directing to the next nearest Na atoms. The NaCl (100) surface is slightly corrugated with Na atoms relaxed inward and Cl atoms relaxed outward, except for the Na atom below the C−C bond which relaxes out of the bulk. Excitation into the S_1 state requires a vertical excitation energy of 6.69 eV according to MSINDO-sCIS. This excitation leads to a rearrangement of the electrons in the molecule. The electrons are transferred from the hydrogen atoms to the carbon atoms, which increases the electron density in the π^* orbital. The following process can be easily understood in the MO picture. Due to the higher population of antibonding π^* orbitals, the first π bond breaks. This population of antibonding orbitals leads to a rehybridization from

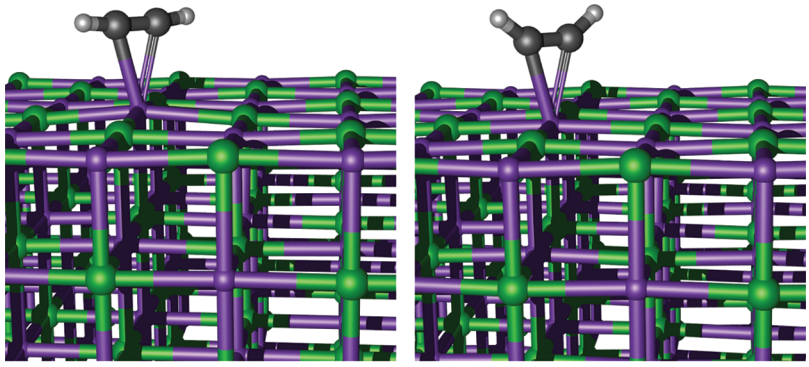

(a) (b)

Figure 3. Overview of the excited state relaxation of adsorbed ethyne at the NaCl (100) surface. (a) The groundstate and (b) the S_1 state. The ∠(CCH) angles are decreased significantly.

dx.doi.org/10.1021/ct200867n | J. Chem. Theory Comput. 2012, 8, 986−996

Table 7. Structural Parameters of the Adsorbed Ethyne for the Ground (GS) and the First Excited State (S_1) and the Changes (Δz) of the Surface Atoms around the Adsorption Site

parameter	GS	S_1	atom	Δz [Å]	atom	Δz [Å]
d_{C-C} [Å]	1.332	1.340	Cl_{Hx}	+0.005	Na_{C-C}	−0.010
d_{C-H} [Å]	1.013	1.085	Cl_{Hy}	+0.006	Na_{C-H}	−0.033
d_{C-Na} [Å]	2.445	2.420				
∠(CCH) [deg]	173.5	144.6				

sp to sp^2 connected with a decrease of the ∠(CCH) by 28.9°. At the same time, the C−C bond is increased. Since the electron density is removed from the C−H bond, this bond is weakened and the interatomic distance is increased by 0.072 Å (additional structural parameters are given in Table 7). The resulting adiabatic energy is 1.66 eV below the vertical excitation energy (E_{0-0} = 5.031 eV, compared to 5.303 eV for the C_{2v} symmetric free gas phase molecule). The change of the adsorbate structure affects the first layer of the NaCl (100) surface (see Table 7). The chlorine atoms relax more out of the bulk by 0.005 Å and 0.006 Å, respectively. The sodium atom below the C−C bond relaxes inward to the bulk (Δz = −0.01 Å). With this effect and the shortening of the C−Na distance, the whole ethyne molecule is nearer to the surface in its first excited state then in the ground state. Similar effects for photoinduced desorption of NO at NiO surfaces have been observed by Baumeister and Freund.[73] There, the laser-induced desorption could be explained by the different potential surfaces of the adsorbed NO at the NiO surface for the excited and ground states. A good overview of related work is given in ref 74. In all previous studies, no periodic boundary conditions have been applied, which leads to large cluster models, which had to be taken into account for this study. This calculation demonstrates the wide range of applicability of the MSINDO-sCIS-CCM method with the implementation of analytical gradients. Here, we provide an alternative way to calculate such photodesorption processes with periodic boundary conditions. In future work, surface catalyzed photoreactions can be studied in detail by optimizing reactands, intermediates, and transition states on excited-state hypersurfaces.

6. SUMMARY AND CONCLUSIONS

We present a study on the implementation and performance of the MSINDO-sCIS and MSINDO-UCIS methods for excited state geometries and adiabatic excitation energies for $\pi-\pi^*$ and $n-\pi^*$ valence excitations. The implementation is computationally highly efficient in particular for larger molecules. Gradient calculations with MSINDO-sCIS/UCIS are 10^3-10^4 times faster than with TD-DFT. This opens a new way to simulate photochemical processes for large and complex systems and the calculation of vibronically coupled optical spectra.

To assess the quality of our method, we have selected a well-studied benchmark set, where highly accurate data obtained with CASPT2 were available. This benchmark set of 10 small and medium sized molecules has been used for an excessive testing of different TD-DFT functionals before.[62] Our MSINDO-sCIS calculations show an accuracy comparable to TD-B3LYP. For adiabatic excitation energies, MSINDO-sCIS is even slightly better than TD-B3LYP in all statistical aspects. C−C and C═C bonds can be calculated with high accuracy, while the C═O bonds are slightly worse compared to TD-B3LYP.

Unfortunately, no such large benchmark set for open-shell molecules is present in the literature. Therefore, we decided to test only two peroxylene radicals in their first two excited states, since those MCSCF results were known. The results were—due to the lack of radicalic peroxy bonds in the reference set, which was used in the parametrization of MSINDO—of medium quality. While the first excited states of both molecules were described with only small errors, the decription of higher states failed qualitatively and quantitatively for all bond lengths or angles including oxygen atoms. We conclude that the large errors are mainly due to spin contamination in the UCIS wave function.

As a last example, we investigated the photoexcitation of ethyne on the NaCl (100) surface. We calculated the geometries of both—the surface and the adsorbed species—in the excited state and discussed the differences from the gas phase. Additionally, we discussed our results with respect to the previously described laser-induced desorption of smaller molecules on oxide surfaces. The MSINDO-sCIS-CCM approach provides an alternative way to large cluster models.

■ ASSOCIATED CONTENT

Supporting Information

Detailed description of the calculation of the analytical gradients for MSINDO-sCIS and MSINDO-UCIS, calculation of the MSINDO-sCIS-Lagrangian and the corresponding CPHF σ vector, calculation of the MSINDO-UCIS-Lagrangian and the corresponding CPHF σ vector, and ground-state geometries. This information is available free of charge via the Internet at http://pubs.acs.org.

■ AUTHOR INFORMATION

Corresponding Author

*E-mail: gadaczek@thch.uni-bonn.de.

Notes

The authors declare no competing financial interest.

■ ACKNOWLEDGMENTS

We would like to thank the Deutsche Forschungsgemeinschaft for the financial support for this work within the Collaborative Research Center SFB 813: Chemistry at Spin Centers, project A2. Additionally, we want to thank Prof. Dr. Frank Neese for his support in the derivation of the equations for analytical ab intio CIS gradients in terms of configuration state functions.

■ REFERENCES

(1) Laane, J. *Structure and Dynamics of Electronic Excited States*; Springer: Berlin, 1999; pp 137−316.
(2) Klessinger, M.; Michl, J. *Excited States and Photochemistry of Organic Molecules*; VCH: Weinheim, Germany, 1995; pp 361−484.
(3) Serrano-Andrés, L.; Merchán, M. *THEOCHEM* **2005**, *729*, 99−108.
(4) Christie, M. R. *Colour Chemistry*; The Royal Society of Chemistry: Cambridge, UK, 1971; pp 379−576.
(5) Christiansen, O.; Koch, H.; Jorgensen, P. *Chem. Phys. Lett.* **1995**, *243*, 409−418.

(6) Christiansen, O.; Koch, H.; Jorgensen, P. *J. Chem. Phys.* **1995**, *103*, 7429−7441.
(7) Koch, H.; Christiansen, O.; Jorgensen, P.; de Meras, A. M. S.; Helgaker, T. *J. Chem. Phys.* **1997**, *106*, 1808−1818.
(8) Schreiber, M.; Silva-Junior, M.; Sauer, S.; Thiel, W. *J. Chem. Phys.* **2008**, *128*, 134110.
(9) Silva-Junior, M. R.; Sauer, S. P.; Schreiber, M.; Thiel, W. *Mol. Phys.* **2010**, *108*, 453−465.
(10) Finley, J.; Malmqvist, P.-A.; Roos, B. O.; Serrano-Andrés, L. *Chem. Phys. Lett.* **1998**, *288*, 299−306.
(11) Buenker, R. J.; Peyerimhoff, S. D.; Butscher, W. *Mol. Phys.* **1978**, *35*, 771−791.
(12) Chattopadhyay, S.; Pahari, D.; Mahapatra, U.; Mukherjee, D. *Comput. Chem.: Rev. Curr. Trends* **2005**, *9*, 121.
(13) Runge, E.; Gross, E. K. U. *Phys. Rev. Lett.* **1984**, *52*, 997.
(14) Grimme, S. Calculation of the Electronic Spectra of Large Molecules. In *Reviews in Computational Chemistry*; John Wiley & Sons, Inc.: New York, 2004; pp 153−218.
(15) Dreuw, A.; Head-Gordon, M. *Chem. Rev.* **2005**, *105*, 4009−4037.
(16) Casida, M. E. *THEOCHEM* **2009**, *914*, 3−18.
(17) Dreuw, A.; Weisman, J. L.; Head-Gordon, M. *J. Chem. Phys.* **2003**, *119*, 2943−2946.
(18) Grimme, S.; Neese, F. *J. Chem. Phys.* **2007**, *127*, 154116.
(19) Goerigk, L.; Moellmann, J.; Grimme, S. *Phys. Chem. Chem. Phys.* **2009**, *11*, 4611−4620.
(20) Tozer, D. J. *J. Chem. Phys.* **2003**, *119*, 12697.
(21) Peach, M.; Benfield, P.; Helgaker, T.; Tozer, D. *J. Chem. Phys.* **2008**, *128*, 044118.
(22) Thiel, W. Semiempirical quantum-chemical methods in computational chemistry. In *Theory and Applications of Computational Chemistry*; Dykstra, C. E., Frenking, G., Kim, K. S., Scuseria, G. E., Eds.; Elsevier: Amsterdam, 2005; pp 559−580.
(23) Jug, K. *Theor. Chim. Acta* **1969**, *14*, 91−135.
(24) Bredow, T.; Jug, K. *MSINDO*. In *Electronic Encyclopedia of Computational Chemistry (online ed.)*; John Wiley & Sons, Ltd.: Chichester, U.K., 2004; DOI: 10.1002/0470845015.cu001.
(25) Bredow, T.; Jug, K. Methods and Techniques in Computational Chemistry, METECC95. In *Methods and Techniques in Computational Chemistry, METECC95*; Clementi, G. E. C., Corongiu, E., Eds.; STEF: Cagliari, 1995; p 89.
(26) Ahlswede, B.; Jug, K. *J. Comput. Chem.* **1999**, *20*, 563−571.
(27) Ahlswede, B.; Jug, K. *J. Comput. Chem.* **1999**, *20*, 572−578.
(28) Bacon, A. D.; Zerner, M. C. *Theor. Chim. Acta* **1979**, *53*, 21−54.
(29) Pople, J. A.; Beveridge, D. L. *Approximate Molecular Orbital Theory*; McGraw-Hill Book Company: New York, 1970.
(30) Ridley, J.; Zerner, M. C. *Theor. Chim. Acta* **1973**, *32*, 111−134.
(31) Gadaczek, I.; Krause, K.; Hintze, K. J.; Bredow, T. *J. Chem. Theor. Comput.* **2011**, *7*, 3675−3685.
(32) Head-Gordon, M.; Rico, R.; Oumi, M.; Lee, T. *Chem. Phys. Lett.* **1994**, *219*, 21−29.
(33) Head-Gordon, M.; Oumi, M.; Maurice, D. *Mol. Phys.* **1999**, *96*, 593−602.
(34) Bredow, T.; Geudtner, G.; Jug, K. *J. Comput. Chem.* **2001**, *22*, 89−101.
(35) Gadaczek, I.; Hintze, K. J.; Bredow, T. *Phys. Chem. Chem. Phys.* **2012**, *14*, 741−750.
(36) Fuchs, F.; Furthmüller, J.; Bechstedt, F.; Shishkin, M.; Kresse, G. *Phys. Rev. B* **2007**, *76*, 115109.
(37) Shishkin, M.; Marsman, M.; Kresse, G. *Phys. Rev. Lett.* **2007**, *99*, 246403.
(38) Brooks, B. R.; Laidig, W. D.; Saxe, P.; Goddard, J. D.; Yamaguchi, Y.; Schaefer, H. F., III. *J. Chem. Phys.* **1980**, *72* (8), 4652−4653.
(39) Krishnan, R.; Schlegel, H. B.; Pople, J. A. *J. Chem. Phys.* **1980**, *72*, 4654−4655.
(40) Osamura, Y.; Yamaguchi, Y.; Schaefer, H. F. III. *J. Chem. Phys.* **1981**, *75*, 2919−2922.
(41) Shepard, R.; Lischka, H.; Szalay, P. G.; Kovar, T.; Ernzerhof, M. *J. Chem. Phys.* **1992**, *96*, 2085−2098.
(42) Shepard, R. *Int. J. Quantum Chem.* **1987**, *31*, 33−44.
(43) Rice, J.; Amos, R. *Chem. Phys. Lett.* **1985**, *122*, 585−590.
(44) Dalgarno, A.; Stewart, A. L. *Proc. R. Soc. London, Ser. A* **1958**, *247*, 245−259.
(45) Handy, N. C.; Schaefer, H. F. III. *J. Chem. Phys.* **1984**, *81*, 5031−5033.
(46) Dalgarno, A.; Stewart, A. L. *Proc. R. Soc. London, Ser. A* **1958**, *247*, 245−259.
(47) Handy, N. C.; Schaefer, H. F. III. *J. Chem. Phys.* **1984**, *81*, 5031−5033.
(48) Dewar, M. J. S.; Thiel, W. *J. Am. Chem. Soc.* **1977**, *99*, 4899−4907.
(49) Patchkovskii, S.; Koslowski, A.; Thiel, W. *Theor. Chem. Acc.* **2005**, *114*, 84−89.
(50) Foresman, J. B.; Head-Gordon, M.; Pople, J. A.; Frisch, M. J. *J. Phys. Chem.* **1992**, *96*, 135−149.
(51) Maurice, D.; Head-Gordon, M. *Int. J. Quantum Chem.* **1995**, *56*, 361−370.
(52) Shroll, R.; Edwards, W. *Int. J. Quantum Chem.* **1997**, *63*, 1037−1049.
(53) Freund, R. W. *SIAM J. Sci. Comput.* **1993**, *14*, 470−482.
(54) Blackford, L. S.; et al. *ACM Trans. Mat. Software* **2002**, *28*, 135−151.
(55) Dongarra, J. J. *Int. J. High Perform. Appl. Supercomput.* **2002**, *16*, 1−199.
(56) Davidson, E. R. *J. Comput. Phys.* **1975**, *17*, 87−94.
(57) Leininger, M. L.; Sherrill, C. D.; Allen, W. D.; Schaefer, H. F. S. III. *J. Comput. Chem.* **2001**, *22*, 1574−1589.
(58) Petrenko, T.; Krylova, O.; Neese, F.; Sokolowski, M. *New J. Phys.* **2009**, *11*, 015001.
(59) Petrenko, T.; Kossmann, S.; Neese, F. *J. Chem. Phys.* **2011**, *134*, 4116.
(60) Page, C. S.; Olivucci, M. *J. Comput. Chem.* **2003**, *24*, 298−309.
(61) Valsson, O.; Filippi, C. *J. Chem. Theory Comput.* **2010**, *6*, 1275−1292.
(62) Guido, C. A.; Jacquemin, D.; Adamo, C.; Mennucci, B. *J. Phys. Chem. A* **2010**, *114*, 13402−13410.
(63) Murrell, J. N.; Harget, A. J. *Semi-Empirical Self-Consistent-Field Molecular Orbital Theory of Molecules*; John Wiley & Sons: New York, 1972; pp 34−120.
(64) Silva-Junior, M. R.; Schreiber, M.; Sauer, S. P. A; Thiel, W. *J. Chem. Phys.* **2008**, *129*, 104103.
(65) Ipatov, A.; Cordova, F.; Doriol, L.; Casida, M. *THEOCHEM* **2009**, *914*, 60−73.
(66) Krauss, M.; Osman, R. *J. Phys. Chem.* **1995**, *99*, 11387−11391.
(67) Krylov, I., A. *Chem. Phys. Lett.* **2001**, *350*, 522−530.
(68) Luzanov, A. V.; Zhikol, O. A. *Int. J. Quantum Chem.* **2010**, *110*, 902−924.
(69) Casanova, D.; Slipchenko, L. V.; Krylov, A. I.; Head-Gordon, M. *J. Chem. Phys.* **2009**, 130 .
(70) Casanova, D.; Head-Gordon, M. *Phys. Chem. Chem. Phys.* **2009**, *11*, 9779−9790.
(71) Huber, K. P.; Herzberg, G. *Molecular Spectra and Molecular Structure*; Van Nostrand Reinhold: New York.
(72) Furche, F.; Ahlrichs, R. *J. Chem. Phys.* **2002**, *117*, 7433−7447.
(73) Baumeister, B.; Freund, H.-J. *J. Phys. Chem.* **1994**, *98*, 11962−11968.
(74) Klüner, T. *Prog. Surf. Sci.* **2010**, *85*, 279−345.
(75) Aikens, C. M.; Webb, S. P.; Bell, R. L.; Fletcher, G. D.; Schmidt, M. W.; Gordon, M. S. *Theor. Chem. Acc.* **2003**, *110*, 233−253.
(76) Schulz, J.; Iffert, R.; Jug, K. *Int. J. Quantum Chem.* **1985**, *27*, 461−464.